SAND2018-9250C

Effect of Flux on the Defects and Electrical Behavior in Si Devices irradiated with He Ions

B. A. Aguirre, G. Vizkelethy, B. Vaandrager, W. J. Martin, P. Seidl, A. Persaud, Q. Ji, B. A. Ludewigt, T. Schenkel and E. Bielejec

Abstract— **We report on the effects of varying the ion flux over eight orders of magnitude using three Si semiconductor devices types under He irradiation. These devices cover a range of doping from 10^{12} to 10^{17} atoms/cm^3 and we used four metrics (diode leakage current, charge collection efficiency, delta inverse gain and deep level transient spectroscopy) to explore the effects of flux on irradiation damage. The key observation was that high fluence irradiations produced less late-time damage due to elevated temperatures from ion beam heating during the irradiation itself.**

Index Terms— **Si diode, BJT, diode leakage current, charge collection efficiency, DLTS, ion irradiation, flux and displacement damage**

I. Introduction

For many years the Ion Beam Lab (IBL) at Sandia National Laboratories (SNL) has used ion beams to simulate displacement damage produced by fast neutron irradiations [1-4]. Metrics such gain degradation, carrier lifetime and types and number of defects have been matched between neutron and ion beam irradiations. However, all the irradiations have been made within a small range of ion fluxes using a variation of ion species including helium, carbon, silicon, germanium, and oxygen beams on Si and GaAs devices. Little or no work has been made on the effect of ion flux on the neutron-ion equivalency. In this work we explored the effects of changing ion flux over eight orders of magnitude on the electrical behavior and defect spectra of Si semiconductor devices

We used the three accelerators shown in Figure 1 to explore the effect of ion flux on the electrical behavior and defect spectra of semiconductor devices. For low flux irradiations we used the National Electrostatic Corporation 3 MV Pelletron and the High Voltage Engineering 6 MV EN Tandem accelerators at SNL. For the high flux irradiations the Neutralized Drift Compression Experiment (NDCX-II) at Lawrence Berkeley National Laboratories (LBNL) [5] was used. While the combination of the Pelletron and Tandem accelerators can irradiate most of the elements in the periodic table with energies up to 3 MeV and ~100 MeV respectively; NDCX-II is limited to H, He and Li ions and a maximum energy of ~1.1 MeV. In this work, we used 1.1 MeV He irradiations as we wanted to perform end-of-range irradiations in Si based semiconductor devices with the same particle mass and energy using all three accelerators. Irradiations made with the Pelletron accelerator delivered a constant flux of $1x10^{11}$ ions/cm^2/s using a constant DC beam. We controlled the fluence with the Pelletron by measuring the charge delivered into the device. Irradiations performed with the Tandem accelerator delivered a constant ion flux of ~$2x10^{14}$ ions/cm^2/s using pulse irradiation with variable pulse lengths from 20 ns up to 100 μs [1]. The fluence was determined by the length and number of the irradiation pulses. Irradiations performed with NDCX-II had a fixed pulse length of ~ 10 ns. This required a change in the ion flux or number of pulses to vary the ion fluence on target. For single shot irradiations, the higher the fluence the higher the ion flux. The maximum flux at NDCX-II was $1.5x10^{19}$ ions/cm^2/s. Using these three accelerators allowed us to explore the effects of ion flux over a maximum of eight orders of magnitude between the Pelletron and NDCX-II irradiations.

II. Experimental Details

We irradiated three types of devices with all three accelerators to explore the effect of ion flux on their electrical performance: Hamamatsu S5821 PIN diodes, S2386 pn diodes and Microsemi 2N2907 pnp BJT transistors. The key difference between these devices was the doping concentration and the resulting location of the ion irradiation damage relative to the built-in depletion depths in each of the devices. The S5821 PIN diode were our lowest doped devices with a doping of 10^{12} atoms/cm^3 we will refer to these as the low doped device. The

Manuscript received August X, 2018. Sandia National Laboratories is a multimission laboratory managed and operated by National Technology and Engineering Solutions of Sandia LLC, a wholly owned subsidiary of Honeywell International Inc. for the U.S. Department of Energy's National Nuclear Security Administration under contract DE-NA0003525.

B. A. Aguirre is with Sandia National Laboratories, Albuquerque, NM 87185 USA (505-844-7302; fax: 505-844-7775; e-mail: baaguir@sandia.gov).

B. Vaandrager is with Sandia National Laboratories, Albuquerque, NM 87185 USA (e-mail: bvaandr@sandia.gov).

G. Vizkelethy is with Sandia National Laboratories, Albuquerque, NM 87185 USA (e-mail: gvizkel@sandia.gov).

W. J. Martin is with Sandia National Laboratories, Albuquerque, NM 87185 USA (e-mail: wjmarti@sandia.gov).

P. Seidl is with Lawrence Berkeley National Laboratories, Berkeley, CA 94720 USA (e-mail: paseidl@lbl.gov).

A. Persaud is with Lawrence Berkeley National Laboratories, Berkeley, CA 94720 USA (e-mail: apersaud@lbl.gov).

Q. Ji is with Lawrence Berkeley National Laboratories, Berkeley, CA 94720 USA (e-mail: qji@lbl.gov).

B. A. Ludewigt is with Lawrence Berkeley National Laboratories, Berkeley, CA 94720 USA (e-mail:).

T. Schenkel is with Lawrence Berkeley National Laboratories, Berkeley, CA 94720 USA (e-mail: t_schenkel@lbl.gov).

E. Bielejec is with Sandia National Laboratories, Albuquerque, NM 87185 USA (e-mail: esbiele@sandia.gov).

S2386 pn diodes were doped at a level of ~10^{15} atoms/cm^3 – we will refer to these as the medium doped devices. Finally, the base doping of the 2N2907 was 10^{17} atoms/cm^3- we will refer to this as the high doped devices. Doping concentration determines the depth of the built-in depletion. By varying the doping concentration, we can vary the location of the 1.1 MeV He ion beam damage relative to the built-in depletion depth. Figure 2 shows optical pictures of the devices used in this study, as well as, a schematics view, not to scale, of the position of maximum ion beam damage in red with respect to the built-in depletion region of each device (shaded area). Figure 2a shows that for the low doped device the built-in depletion region is very wide and the damage produced by the He ions is completely localized inside the built-in depletion region. Figure 2b shows that for the medium doped device the damage peak is placed outside the built-in depletion region; however, we can apply an external voltage to probe the damaged region. Finally, Figure 2c shows the damage peak, targeting the base-emitter (BE) junction, covered a wider region than the entire built-in depletion width for the high doped devices. The location of the built-in depletion layer versus the ion beam damage will affect the type of metric we use to explore the high flux radiations.

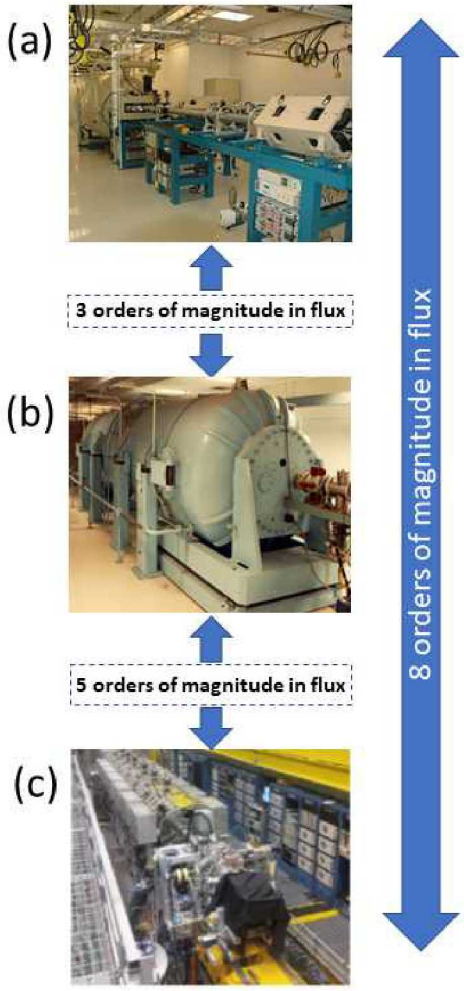

Figure 1 shows the three accelerators used in this work to explore the effect of ion flux on electrical performance and defect creation: a) Pelletron, b) Tandem and c) NDCX-II.

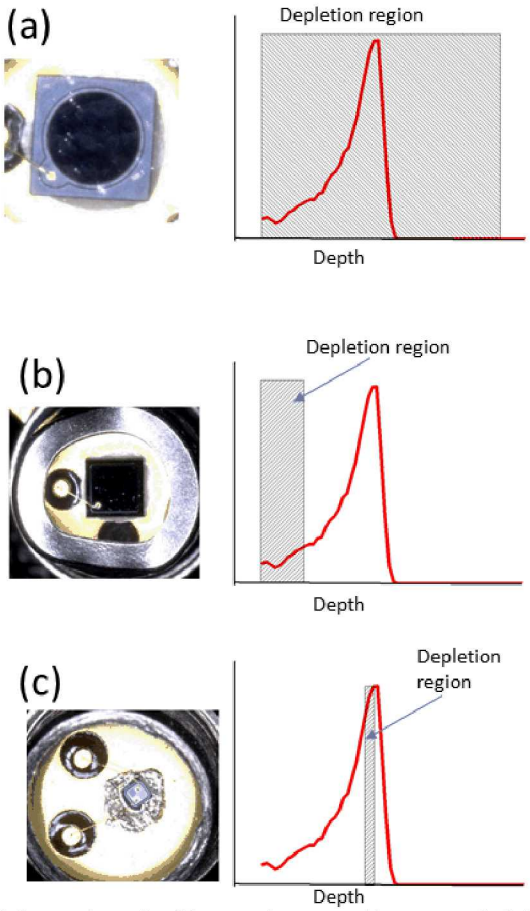

Figure 2 shows schematic of damage placement with respect to built-in depletion width for a) low doped, b) medium doped and c) highly doped devices.

We used four metrics shown in Figure 3 to study the effect of ion flux on the electrical performance and defect spectra of the low, medium and highly doped devices: diode leakage current, charge collection efficiency (CCE), delta inverse gain (DIG) and deep level transient spectroscopy (DLTS) [6]. Leakage current measures global damage and is proportional to the number of defects. We performed leakage current measurements from 0 – 20 V on the PIN and pn diodes irradiated with 0.5x10^{12} to 2x10^{12} fluence levels and after an ASTM [7] annealing (80 °C for two hours) after irradiation using either the Pelletron (low flux) or NDCX-II (high flux). CCE measurements were performed with an ion beam induced charge (IBIC) setup in which devices under test were first irradiated to high fluence values using the 1.1 MeV He beam to create the damage and then probed with a 2 MeV He beam. Here the probing fluence is always much lower than the damaging fluence to ensure we are measuring the effects of the 1.1 MeV He irradiation. The inset of Figure 3b shows ionization profile of the 2 MeV He probing beam with respect to the 1.1 MeV He damage profile. The role of the probing beam is to generate electron-hole pairs that can be collected in the device as a function of bias. The higher the damage produced by the damaging 1.1 MeV He beam, the less charge gets collected from the 2 MeV He probing beam. CCE is proportional to 1 - number of defects and we performed CCE measurements for devices irradiated with fluence values between 0.5x10^{12} to

$2x10^{12}$ ions/cm^2 after they went through an ASTM annealing where:

$$CCE = \frac{Charge\ collected}{Charge\ deposited} \propto 1 - a(\#\ of\ defects) \quad (1)$$

where α is a scaling constant.

We also measured the gain of 2N2907 Si pnp BJTs irradiated to different fluence and flux values to calculate and plot the DIG vs. fluence as shown in Figure 3c where according to the Messenger-Spratt equation [8]:

$$DIG = \frac{1}{G_f} - \frac{1}{G_i} = k\varphi \propto (\#\ of\ defects) \quad (2)$$

where G_f is the final gain, G_i is the initial gain, k is the Messenger-Spratt damage factor and Φ is the ion fluence.

The final metric we used to study the effect of ion flux on semiconductor devices was DLTS as shown in Figure 3d, where we can obtain a defect spectrum of the type of defects present after irradiation and the DLTS amplitude is proportional to the number of traps in a n^+p step junction as follows:

$$\frac{N}{(N_A - N_D)} = 2\left(\frac{\Delta C}{C}\right) \quad (3)$$

where N is the trap concentration, $(N_A - N_D)$ is the acceptor and donor concentrations, ΔC is the capacitance change due to a bias pulse and C is the junction capacitance under quiescent reverse bias [6].

Figure 3d shows an example of the typical DLTS spectrum obtained in Si devices exposed to ion irradiations. The three main DLTS peaks observed in Figure 3d correspond to the vacancy oxygen (VO) peak located at E_C – 0.17eV [9], the shallow di-vacancy ($V_{2(=/-)}$) at E_C – 0.24 eV and the deep peak which consists of the vacancy phosphorous (VP) (in the highly doped n-type based of the Si pnp BJT), the deep divacancy ($V_{2(-/0)}$), the strained di-vacancy (V_2^*) and E5 located at E_C - 0.43 eV [10].

Since DLTS depends on the change of the capacitance due to the change of the depletion region at different bias voltages, the defects created inside the built-in depletion cannot be probed. For the low doped devices, the defects were created inside the built-in depletion region as shown in Figure 2a and therefore DLTS measurements could not be performed on these devices. Table 1 summarizes the characterization techniques applied to each device and their proportionality to the number of defects. his table shows that we had a good overlap between the different device types and the characterization techniques used in this study.

Table 1 summarizes the characterization techniques used in each device for this study.

Characterization	Low Doping	Medium Doping	High Doping	
Leakage current	✓	✓	×	∝ # of defects
CCE	✓	✓	×	∝ 1 – (# of defects)
DLTS	×	✓	✓	∝ # of defects
Gain	×	×	✓	∝ # of defects

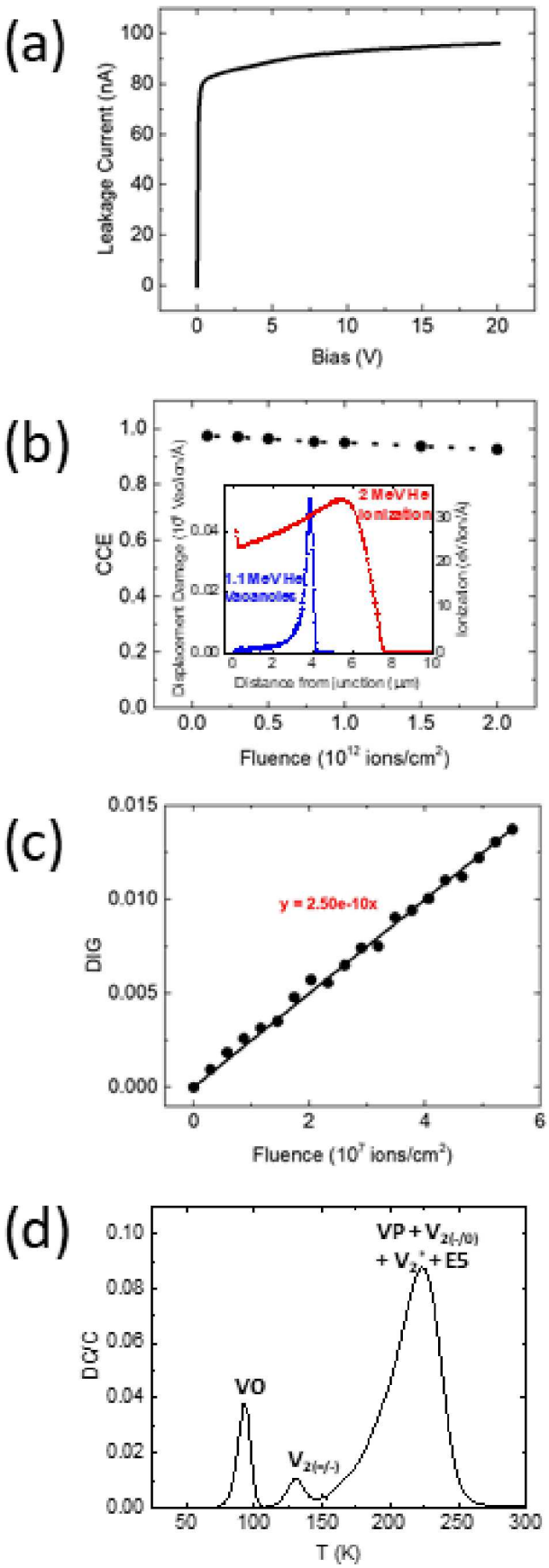

Figure 3 Shows the four metrics used to analyze the effect of ion flux: a) diode leakage current, b) CCE, c) DIG vs fluence and d) DLTS.

III. Results and Discussions

Overall, we find that the NDCX-II high flux irradiations produce less damage and less defects than low flux Pelletron and Tandem irradiations in the low, medium and highly doped devices. Figure 4 shows leakage current and CCE results for low doped PIN diodes that were exposed to a range of fluences under high ($1.5x10^{19}$) and low ($1x10^{11}$) flux conditions. We observe from Figure 4a that low-flux-irradiated PIN diodes had a larger leakage current at 10 V when they were irradiated to the same level of fluence as compared to the high-flux-irradiated diodes. Also, for a fixed fluence of $5x10^{11}$ ions/cm^2, the leakage current at high and lox flux irradiations is independent of the bias voltage in a range from 0 to 20 V as shown in Figure 4b. Figure 4c shows that low flux irradiations also degraded the CCE more than the high flux irradiations. Similar results were obtained for the medium doped S2386 pn diodes in Figure 5 where low flux irradiations produced higher leakage current and higher CCE degradation than low flux shots. Note that the change in the leakage current is greatly reduced in the medium doped devices. The damage is more visible in the low doped devices because the defect to dopant ratio is larger than in medium doped devices (less compensation occurs in the medium doped devices). For example, a fluence of $1x10^{12}$ ions/cm^2 will have a higher effect and possibly compensate devices doped to 10^{12} atoms/cm^3 than devices doped to 10^{15} atoms/cm^3. Figure 5b shows the bias dependence of the CCE as a function of bias voltage. As we have noted the higher doping devices show a much smaller effect. This is also seen with bias conditions. The 0 V condition shows a small, but clear difference between the flux rates, whereas for higher bias (10 V) the difference is masked. Figure 5c shows the DLTS spectra obtained for two pn diodes irradiated to $5x10^{11}$ ions/cm^2 under low and high flux conditions. The high flux conditions produced a smaller DLTS deep peak compared to the low flux irradiation. In addition, the VO peak of the high flux irradiation is larger than the low flux irradiation. The conclusion from all three of these metrics in both the low and medium doped devices is that less defects were created by high flux shots.

We performed gain measurements and probed the base-emitter junction of the highly doped Si BJTs with DLTS to study the effect of ion flux. The DIG data calculated from the gain measurements suggests that the high flux irradiations produce slightly more damage than the low flux case as seen in Figure 6. The slope of the fitting lines represents the damage factor k in equation 2 and we observed that high flux conditions resulted in a 30% higher k-factor compared to low flux irradiations, however, we believe that this difference is due to uncertainty in the fluence calculations and beam targeting on the sample at NDCX-II. A similar analysis with the base current instead of DIG yielded the same results obtained in Figure 6.

DLTS measurements on the same Si BJTs, shown in Figure 7, show the typical DLTS peaks described above. The DLTS spectra for low and high flux irradiations were plotted on the same scale to show the high flux irradiations produced much smaller deep level DLTS peaks; and therefore, less defects than the low flux irradiations for the same gain degradation. This implies that the deep peak in the low flux irradiations contains defects that are not critical to the gain degradation of transistors. This result agrees with a recent study that found that low mass particles produce more VP defects; which have less impact on gain degradation than clustering related defects such as V_2* and E5 [11]. The studies in [11] and [12] showed that when VP anneals, a DLTS peak attributed to VP_2 starts growing in the same position as VO; therefore the present study suggests that the low flux irradiations produce an excess of VP defects compared to the high flux irradiations or that VP defects anneal out during high flux conditions into VP_2.

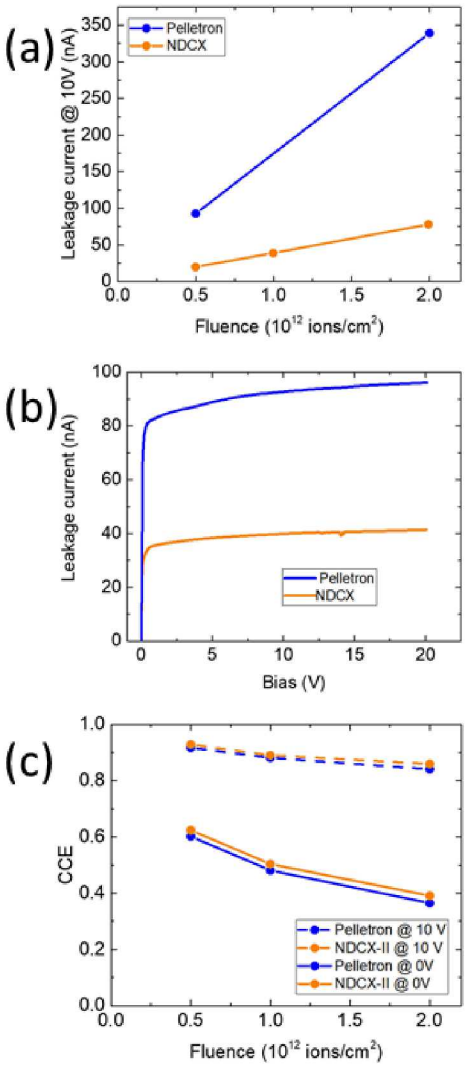

Figure 4 shows a) leakage current at 10 V, b) leakage current vs bias for $5x10^{11}$ ions/cm^2 irradiations and c) CCE for low doped PIN diodes irradiated with high and low ion fluxes.

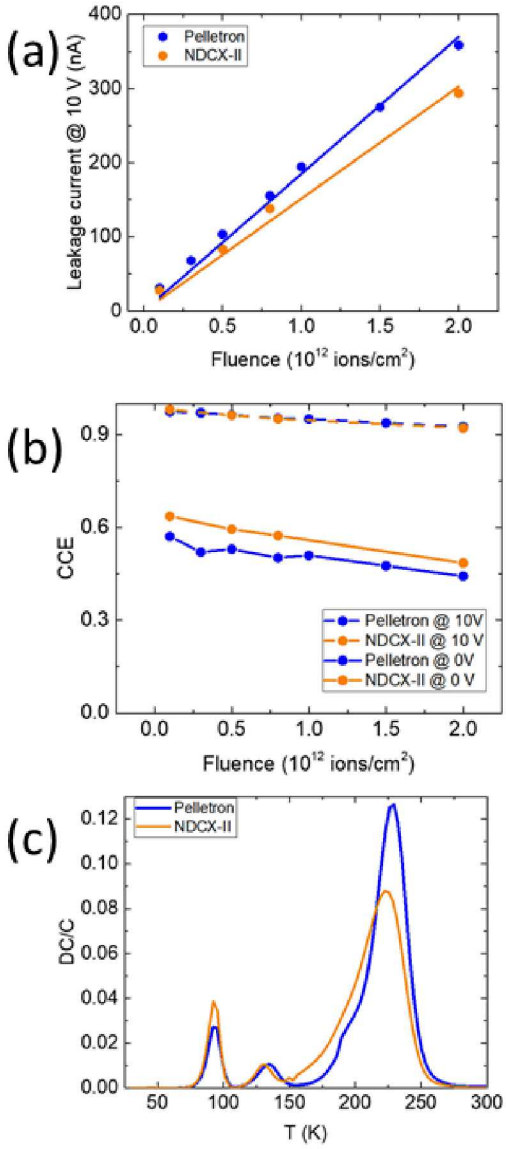

Figure 5 shows a) leakage current at 10 V, b) CCE vs fluence and c) DLTS for medium doped diodes exposed to low and high ion flux irradiations.

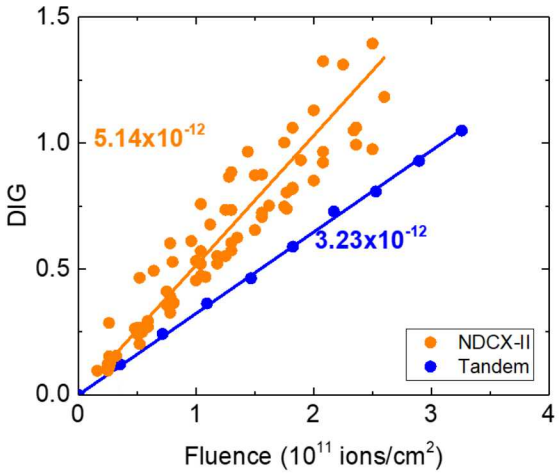

Figure 6 shows the DIG vs fluence for high doped Si BJTs irradiated with low and high flux irradiations.

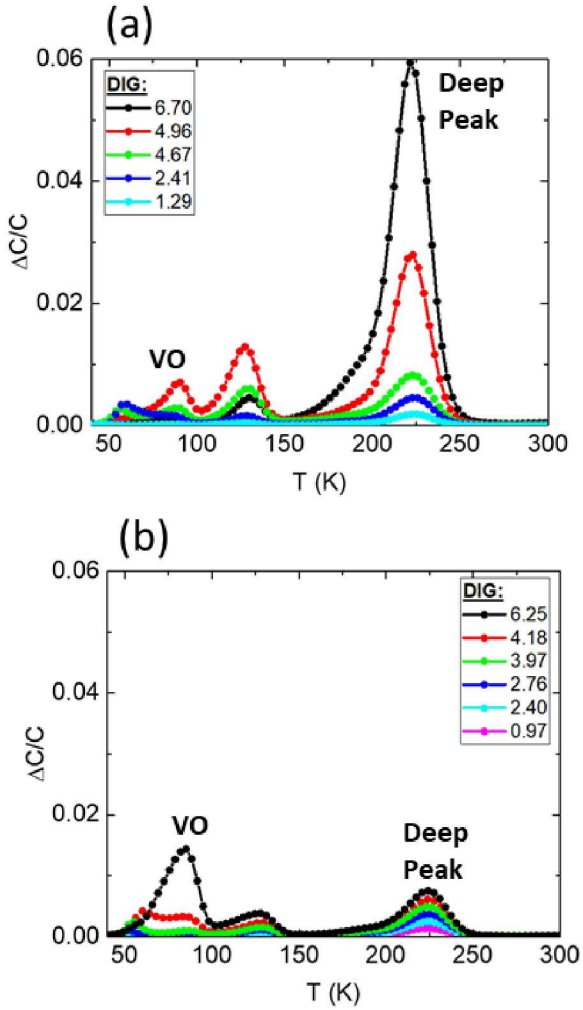

Figure 7 DLTS at the BE junction of devices exposed to a) low and b) high ion flux irradiations for relatively the same gain degradation.

Exploring the DLTS spectra in more detail leads to additional questions, namely, why does the shallow defect levels such as the VO peak at ~90 K for the 1 ms correlator setting in this experiment appear to be much larger under high flux irradiations than low flux irradiations. Typically, the peak amplitude scales linearly with fluence and DIG. In sum, we observed two contradictory effects in the DLTS spectra under high flux irradiations: (1) The VO peak is larger while (2) the deep peak is smaller. This is interesting as it is typically thought that the defects contributing to the deep peak are the dominant recombination centers while the shallow VO plays essentially no role in the DIG or base current changes.

Re-plotting the NDCX-II DLTS spectra of Figure 7 with a different scale in Figure 8 we observe (1) the deep peak height increases linearly with DIG and (2) the VO (VP2) peak increases exponentially with DIG. This is an unexpected result, potentially related to either high damage levels or elevated temperatures. DIG levels of 1-6 indicates that we have dramatically affected transistor operation, however, as mentioned earlier similar results are seen when using changes in the base current in place of DIG. Previous experimental work that suggests that elevated temperature irradiations and annealing can promote the preferential formation of VO defects

[13]. In the NDCX-II irradiations the elevated temperatures maybe due to localized self-heating from the high flux ion irradiation.

To explore these two effects, we performed low flux irradiations under two different scenarios: (1) high fluence irradiations to obtain high damage levels with DIG values similar to the high flux case and (2) low flux irradiations under elevated temperature annealing over a range of fluence values. Here, the transistor was heated to a fixed temperature, kept at this temperature during the ion irradiation (pulse length from 20-200 μs), then the heater was turned off immediately after the shot. For the first scenario, low flux irradiations produced the DLTS peaks shown in Figure 9 where the deep and VO peaks grow non-linearly with DIG. For the second scenario, in-situ annealing irradiations shown in Figure 10 resulted on a decrease of the deep peak and a non-linear increase of the VO peak as in-situ temperature increased.

The results in Figure 10 indicate that deep peak defects (we believe the VP fraction of it) are annealed out under high temperature conditions and they also confirm the results on the VO peak previously observed. However, neither the high damage levels nor the in-situ annealing irradiations explain the results of the high flux NDCX-II irradiations observed in Figure 8. We believe that the NDCX-II results are a combined effect of high damage levels with localized annealing under high flux irradiations as shown in Figure 11. In other words, the non-linear increase of the VO peaks is promoted by localized annealing where the VP decreases but the VO increases. Whereas, the deep peak grows linearly due to competing mechanisms between a non-linear increase due to high damage levels and a non-linear decrease due to localized annealing during high flux irradiations.

Preliminary modeling work [14] shown in Figure 12 suggests that elevated temperatures can occur during high flux irradiations and have the potential of annealing defects and promoting the VO formation as the elevated temperature can last for 1000's of ns. However, the predicted temperatures of ~325 K at the surface and ~320 K at the He end-of-range is insufficient to account for the VO growth from our experimental results. However, we have to note that the simulation was done for the actual current hitting the device (20 mA), which is isolated except the back connected to a room temperature reservoir. Since the beam is much larger and hitting the surrounding sample holder the above assumptions might not be correct and higher temperatures might exist.

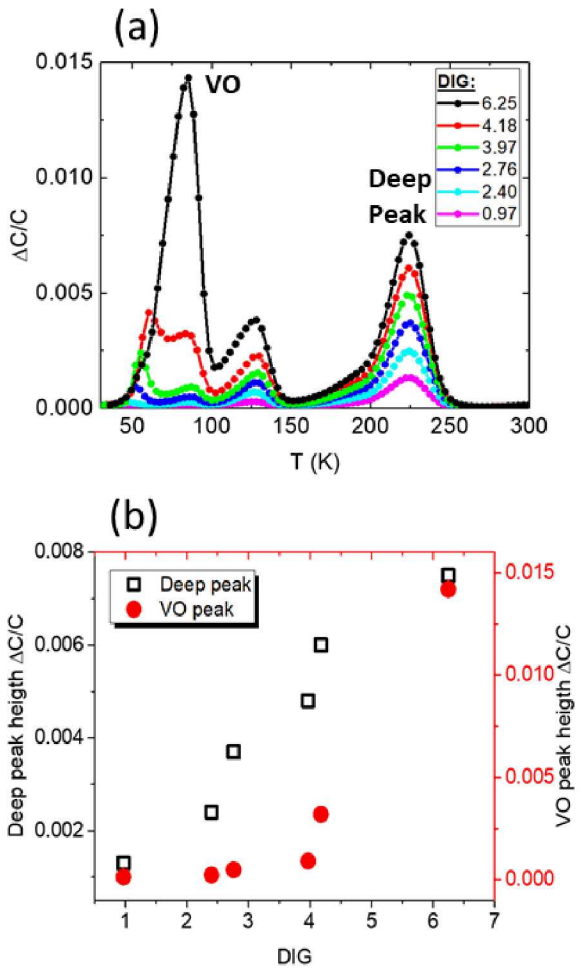

Figure 8 Shows a) DLTS spectra at the BE junction of Si BJTs irradiated to different DIG levels using high flux irradiations and b) the deep and VO DLTS peak heights vs DIG.

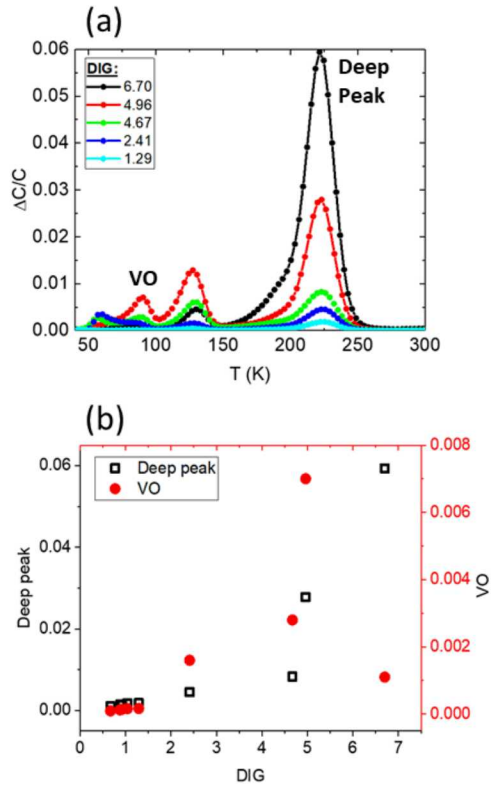

Figure 9 Shows a) DLTS spectra at the BE junction of Si BJTs irradiated to different DIG levels using low flux irradiations and b) the deep and VO DLTS peak heights vs DIG.

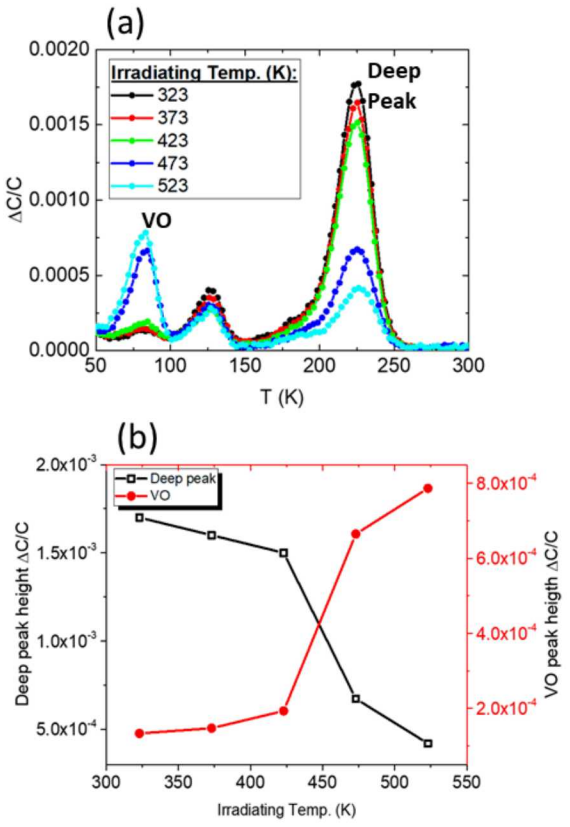

Figure 10 Shows a) DLTS spectra at the BE junction of Si BJTs irradiated with low flux at different temperatures and b) the deep and VO DLTS peak heights vs irradiating temperature.

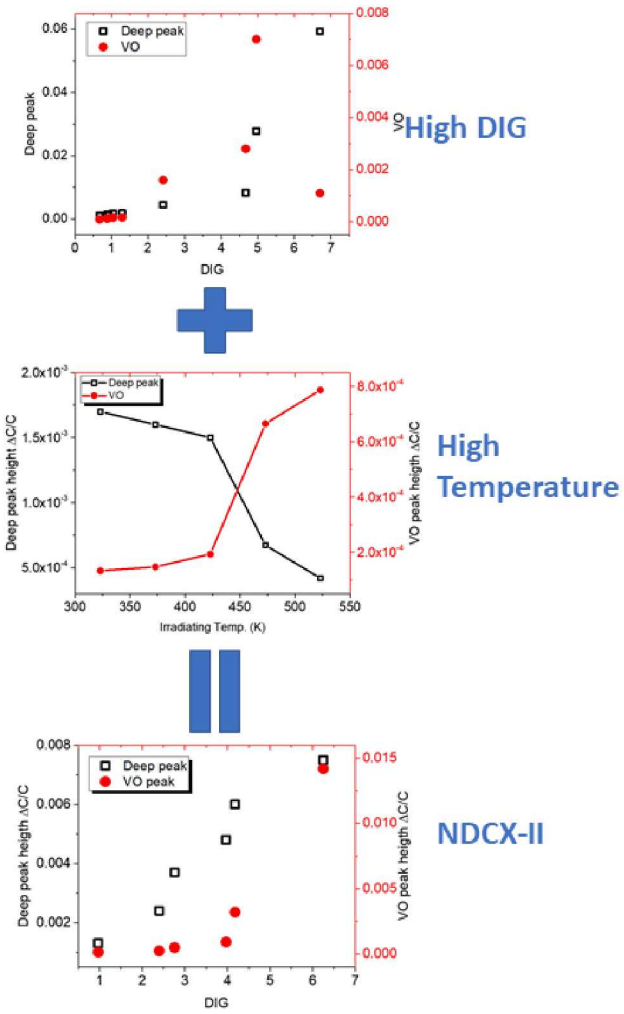

Figure 11 shows the combined mechanisms of high damage levels and temperature that result in the high flux irradiations.

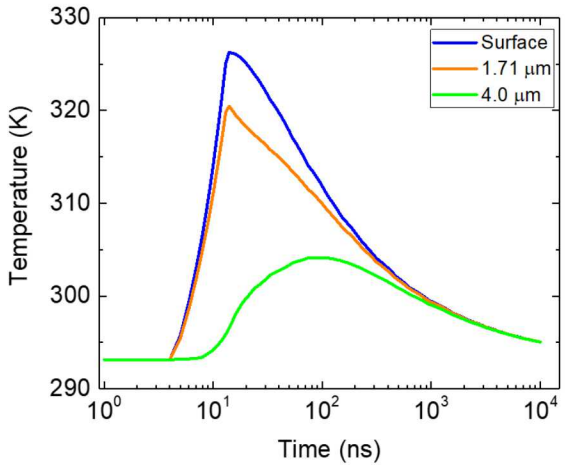

Figure 12 shows preliminary modeling results that suggests we have elevated temperature possible during the high flux irradiations.

IV. CONCLUSIONS

The overall conclusion is that the high flux shots from the NDCX-II facility result in less damage in the irradiated devices as the elevated temperature present during the ion beam irradiation acts to locally anneal out the VP defect and promote the VO formation. This is observed in three of the four metrics and in all the tested devices (low, medium and high doping levels). We found that the difference in the effect of the flux difference (apart from DLTS) strongly depends on the doping level, higher the doping smaller the effect is. As mentioned the most straightforward explanation for the DIG results is that the NDCX-II fluence values might have a systematic offset. This is one of the key reasons why we choose to use DIG (or equivalently base current) as our metric in place of fluence when comparing the DLTS spectra. The implications of this for device qualification is that one needs to ensure a complete study of the expected flux conditions to accurately predict the expected change in physical and operational parameters of a device. Note the effect of localized annealing will lead us to overestimate the expected damage levels using low flux simulators.

REFERENCES

[1] E. Bielejec, G. Vizkelethy, R. M. Fleming, and D. B. King, "Metrics for Comparison Between Displacement Damage due to Ion Beam and Neutron Irradiation in Silicon BJTs," *Nuclear Science, IEEE Transactions on,* vol. 54, pp. 2282-2287, 2007.

[2] E. Bielejec, G. Vizkelethy, N. R. Kolb, D. B. King, and B. L. Doyle, "Damage Equivalence of Heavy Ions in Silicon Bipolar Junction Transistors," *Nuclear Science, IEEE Transactions on,* vol. 53, pp. 3681-3686, 2006.

[3] E. Bielejec, G. Vizkelethy, R. M. Fleming, W. R. Wampler, S. M. Myers, and D. B. King, "Comparison between experimental and simulation results for ion beam and neutron irradiation in silicon bipolar junction transistors," *IEEE Transactions on Nuclear Science,* vol. 55, 2008.

[4] E. Bielejec, R. M. Fleming, G. Vizkelethy, J. C. Banks, and D. B. King, "Overview of the QASPR damage relationships and the effects of di-vancancy bistability as measured by gain and DLTS," *Journal of Radiation Effects Research and Engineering,* vol. 28, pp. 7-15, 2010.

[5] P. A. Seidl, "Irradiation of Materials With Short, Intense Ion Pulses at NDCX-II," *Laser and Particle beams,* vol. 35, pp. 373-378, 2017.

[6] D. V. Lang, "Deep-level transient spectroscopy: A new method to characterize traps in semiconductors," *Journal of Applied Physics,* vol. 45, pp. 3023-3032, 1974.

[7] A. S. E1855-05, "Standard Test Method for Use of 2N2222A Silicon Bipolar Transistors as Neutron Spectrum Sensors and Displacement Damage Monitors," vol. 12.02, ed: ASTM International (www.astm.org), 2005.

[8] G. C. Messenger and J. P. Spratt, "The effects of neutron irradiation on germanium and silicon," *Proc. IRE,* vol. 46, pp. 1038-1044, 1958.

[9] R. M. Fleming, C. H. Seager, D. V. Lang, E. Bielejec, and J. M. Campbell, "Gain and defect bi-stability in radiation damaged silicon bipolar transistors," *Physica B: Condensed Matter,* vol. 401-402, pp. 21-24, 2007.

[10] R. M. Fleming, C. H. Seager, D. V. Lang, E. Bielejec, and J. M. Campbell, "A bistable divacancylike defect in silicon damage cascades," *Journal of Applied Physics,* vol. 104, pp. 083702-10, 2008.

[11] B. A. Aguirre, E. Bielejec, R. M. Fleming, G. Vizkelethy, B. Vaandrager, J. Campbell, W. J. Martin and D. B. King, "Comparison of Gain Degradation and Deep Level Transient Spectroscopy in pnp Si Bipolar Junction Transistors Irradiated With Different Ion Species," *IEEE Transactions on Electron Devices,* vol. 64, pp. 190-196, January 2017 2017.

[12] R. M. Fleming, C. H. Seager, E. Bielejec, G. Vizkelethy, D. V. Lang, and J. M. Campbell, "Defect Annealing in Neutron and Ion Damaged Silicon: Influence of Defect Clusters and Doping," *Journal of Applied Physics,* vol. 107, p. 053712, 2010.

[13] V. P. Markevich, A. R. Peaker, S. B. Lastovskii, V. E. Gusakov, I. F. Medvedeva, and L. I. Murin, "Formation of Radiation-Induced Defects in Si Crystals Irradiated with Electrons at Elevated Temperatures," *Solid State Phenomena,* vol. 156-158, pp. 299-304, 2009.

[14] ""COMSOL: Multiphysics Modeling and Simulation." from www.comsol.com."